

## An Ultrasonication-Assisted Extraction and Derivatization Protocol for GC/TOFMS-Based Metabolite Profiling

By: Yumin Liu, Tianlu Chen, Yunpin Qiu, Yu Cheng, Yu Cao, Aihua Zhao, and Wei Jia

Liu, Y.M., Chen, T.L., Qiu, Y.P., Cheng, Y., Cao, Y., Zhao, A.H., Jia, W. (2011). An ultrasonication-assisted extraction and derivatization protocol for GC/TOFMS-based metabolite profiling, *Analytical and Bioanalytical Chemistry*, 400(5), 1405-1417.

**\*\*\*Note: This version of the document is not the copy of record. Made available courtesy of Springer Verlag. The original publication is available at [www.springerlink.com](http://www.springerlink.com).  
Link to Article: <http://www.springerlink.com/content/1q8353g821421380/>**

### **Abstract:**

Conventional chemical derivatization of metabolites in biological specimens is time-consuming, which limits the throughput and efficiency of metabolite profiling using a gas chromatography/time-of-flight mass spectrometry (GC/TOFMS) platform. We report an ultrasonication-assisted protocol which reduces the derivatization time from hours to about 30 min and significantly enhances the derivatization efficiency prior to a GC/TOFMS analysis. The protocol was evaluated using 40 compounds representing different classes of human metabolites, and demonstrated good analytical precision and accuracy. In comparison with the conventional method, the new protocol was able to increase the intensity of most of the identified peaks (71.0%) in the GC/TOFMS chromatograms of human serum samples. The detected compounds with increased intensity include most amino acids, keto-containing organic acids, carbonyl-containing carbohydrates, and unsaturated fatty acids. We applied this protocol in a metabolomic study of human serum samples obtained from 34 patients diagnosed with hypertension and 29 age- and gender-matched healthy subjects. Metabolite markers associated with hypertension, including glucosamine, D-sorbitol, 1-stearoylglycerol, and homocysteine, were identified and validated by statistical methods and use of reference standards. Our work highlights the potential of this novel approach for the large-scale metabolite profiling of samples generated from plant, animal, and clinical and epidemiological studies.

### **Article:**

#### **INTRODUCTION**

Metabonomics or metabolomics emerged following genomics, transcriptomics, and proteomics as an approach for capturing global biochemical alterations associated with pathophysiological changes [1–3]. To date, various analytical approaches, such as proton nuclear magnetic resonance, liquid chromatography/mass spectrometry (LC/MS), and gas chromatography/mass spectrometry (GC/MS), are employed to detect the variations of low molecular mass metabolites (less than 1,000 Da) in biological samples (e.g., urine, blood, tissue, cell, organs) [4–6]. LC/MS can analyze a wide range of chemical species that are not volatile and do not need chemical derivatization. As a result, LC/MS is best suited for the measurement of targeted metabolites that are not readily amenable to GC/MS analysis because of volatility issues. As one of the analytical

approaches frequently used in metabolomic studies, GC/MS exhibits satisfactory sensitivity and good resolution. Together with the sample derivatization method, GC/MS can detect the volatile or nonvolatile compounds, or both, in various sample matrices [7, 8]. Presently, the silylation approach is the preferred and widely used derivatization method for GC/MS-based metabolomic studies of diseases such as diabetes [9], hypertension [10], and colorectal cancer [11]. Since there is abundant biological information on amines, amino acids, organic acids, fatty acids, carbohydrates, vitamins, and phospholipids in biological samples, careful consideration should be given to factors which could affect the measurement of the global metabolites in GC/MS analysis [12, 13]. One of the most important considerations for the silylation method selected is its applicability to various metabolites in the biological sample. Metabolites in a given biological specimen differ widely from each other in chemical nature and amounts; therefore, the derivatization conditions of different metabolites, such as silylating reagent, reagent concentration, reaction time, temperature, and solvents, need to be optimized to maximize the number of metabolites of interest detected in a metabolomic study. Another factor to be considered is that the derivatization treatment for most metabolites usually requires a long reaction time up to 20 h [11, 13]. When simultaneously used for hundreds of biological samples, the derivatization process of metabolite reaction can be rather time-consuming. Additionally, undesirable side reactions may occur if the derivatization process is too long. Thus, there are many challenges associated with developing a high-throughput and high-efficiency sample preparation method for metabolomic studies.

It has been reported that derivatization reactions can be improved with auxiliary energies, such as microwaves or ultrasound [14, 15]. Microwaves are electromagnetic waves which may readily damage biological specimens [16]. Ultrasound, however, is inexpensive and safe, and the integrity of most biological samples remains unchanged even after a long-term exposure to an ultrasonic energy field. Also, cavitation occurs by the passage of ultrasonic waves through the solvent. The cavitation effect can slightly increase the temperature and pressure, and can promote effective interaction between the substrate and the derivative reagent, and consequently enhance chemical reactions [17]. Ultrasonic derivatization reactions have been effectively used for transesterification, silylation, and glycosylation [18–21]. Fiamegos et al. [22] recently reported a detailed protocol for the esterification of amino acids in urine with the aid of ultrasonic energy. However, no relevant studies have been published to date on metabolomic profiling using ultrasonication for the silylation reaction of the metabolites in biological specimens.

In this study, a high-throughput and high-efficiency ultrasonic derivatization protocol for analyzing endogenous metabolites in serum was developed. Much effort was directed to the optimization of the extraction time, methoxymation, and silylation reaction prior to instrumental analysis. The protocol developed was evaluated using known standard compounds and human serum samples. A clinical metabolomic investigation was designed to test the applicability of this protocol for the profiling of a wide range of serum metabolites that were significantly altered in association with the pathological state of hypertension.

## EXPERIMENTAL

### *Materials and chemicals*

Chromatographic grade methanol, acetonitrile, ethanol, and chloroform were purchased from Merck Chemicals (Germany). All of the chemicals, such as pyridine, methoxyamine, *n*-hexane, and *N,O*-bis(trimethylsilyl)trifluoroacetamide (BSTFA) containing 1% trimethylchlorosilane (TMCS), and the reference standards used in the study were purchased from Sigma-Aldrich (St. Louis, MO, USA). Forty stock solutions, including solutions of amino acids, organic acids, fatty acids, nucleosides, carbohydrates, and cholesterol, were prepared with ultrapure water from a Milli-Q system (Millipore, Billerica, MA, USA) or ethanol and were stored at  $-20\text{ }^{\circ}\text{C}$ . L-2-Chlorophenylalanine at  $0.3\text{ mg mL}^{-1}$  in water and heptadecanoic acid at  $0.1\text{ mg mL}^{-1}$  in ethanol were prepared and used as internal standards (IS).

### *Human sera*

Serum specimens from 34 patients ( $61 \pm 13$  years old, 14 male, 20 female) diagnosed with hypertension and from 29 healthy subjects ( $59 \pm 11$  years old, 12 male, 17 female) were provided by Shanghai Yangpu Center for Disease Control and Prevention. Patient participants were diagnosed according to the Joint National Committee on Prevention, Detection, Evaluation, and Treatment of High Blood Pressure (JNC 7) (established in 2003) and China's prevention and cure guide of hypertension (established in 2004) [23]. This study was approved by the Institutional Review Board of the Shanghai Yangpu Center for Disease Control and Prevention and written informed consent was obtained from all participants. Patients selected had not been using any therapeutic drugs within the last 12 h prior to blood collection. Venous blood samples were collected from patients and healthy volunteers in Eppendorf tubes, after a 12-h overnight fasting period, using all necessary precautions to avoid contamination. The samples were then allowed to clot at room temperature. Sera were then separated by centrifugation at  $3,000\text{ g}$  for 20 min at  $4\text{ }^{\circ}\text{C}$ , and were stored in aliquots at  $-80\text{ }^{\circ}\text{C}$ . All the samples were thawed at room temperature and vortex-mixed before use.

### *Sample preparation*

An aliquot of 100  $\mu\text{L}$  serum sample, 300  $\mu\text{L}$  methanol–chloroform (3:1 v/v), and two IS, L-2-chlorophenylalanine and heptadecanoic acid (in 10  $\mu\text{L}$  of water and ethanol, respectively), were mixed for metabolite extraction, and then kept at  $-20\text{ }^{\circ}\text{C}$  for 10 min. After centrifugation at  $12,000\text{ g}$  for 10 min, 300  $\mu\text{L}$  supernatant was dried completely under nitrogen. Methoxyamine (80  $\mu\text{L}$ ;  $15\text{ mg mL}^{-1}$  in pyridine) was added to the residue to start the methoxymation. Subsequently, the sample was trimethylsilylated by adding *n*-hexane and BSTFA (with 1% TMCS). All samples were analyzed by gas chromatography/time-of-flight mass spectrometry (GC/TOFMS) in randomized order.

### *GC/TOFMS analysis*

GC/TOFMS analysis was performed using an Agilent 6890 gas chromatograph system coupled with a Pegasus III time-of-flight mass spectrometer. The system utilized a DB-5MS capillary column coated with 5% diphenyl cross-linked with 95% dimethylpolysiloxane (30 m  $\times$  250- $\mu\text{m}$  inner diameter, 0.25- $\mu\text{m}$  film thickness; J&W Scientific, Folsom, CA, USA). A 1- $\mu\text{L}$  aliquot of the analyte was injected in splitless mode. Helium was used as the carrier gas, the front inlet purge flow was  $20\text{ mL min}^{-1}$ , and the gas flow rate through the column was  $1\text{ mL min}^{-1}$ . The initial temperature was kept at  $80\text{ }^{\circ}\text{C}$  for 2 min, then raised to  $180\text{ }^{\circ}\text{C}$  at a rate of  $10\text{ }^{\circ}\text{C min}^{-1}$ ,

then to 240 °C at a rate of 5 °C min<sup>-1</sup> and finally to 290 °C at a rate of 25 °C min<sup>-1</sup> for 9 min. The injection, transfer line, and ion source temperatures were 270, 220, and 260 °C, respectively. The energy was 70 eV in electron impact mode. The mass spectrometry data were acquired in full-scan mode with the *m/z* range of 30–550 at a rate of 20 spectra per second after a solvent delay of 360 s.

### *Ultrasonication-assisted procedures*

**Ultrasonicated extraction.** The organic solvent (3:1 methanol–chloroform) was used for serum metabolite extraction. We evaluated the extraction efficiency of the ultrasonic treatment in comparison with the conventional vortex method. A total of 24 tests (including replicates) were performed with different vortex times (2 and 10 min) and different ultrasonic times (1, 2, 3, 4, 5, 6, 10, 15, 20, and 30 min) for metabolite extraction. The ultrasonication was carried out in a KQ-250DB ultrasonic bath (40 kHz, 350 W).

**Ultrasonicated methoxymation.** The methoxymation under ultrasonication was carried out under different conditions as follows: different reaction times (2, 5, 7, 10, 15, 20, 30, 45, and 60 min) with a high-intensity ultrasound field (ultrasonic irradiation at 40 kHz, 350 W). The conventional methoxymation procedure (incubation at room temperature for 90 min or 16 h) was used as a control [13]. Each experimental condition was repeated three times.

**Ultrasonicated silylation.** To optimize the silylation steps, the ultrasonication temperature, time, irradiation power, and silylation volume were evaluated. On the basis of the orthogonal experimental design L<sub>27</sub> (3<sup>13</sup>), a total of 27 ultrasonication-assisted silylation experiments were performed. Another two conventional silylation experiments were conducted as controls. Each run was duplicated (Table 1).

### *Analytical method validation*

With use of the optimized procedure, the linearity of 40 reference standards from different chemical classifications was investigated in the concentration range for the routine metabolic analysis. The linearity of the serum metabolites was also investigated. After the instrumental analysis by GC/TOFMS, the analytical curve was constructed by the peak-area ratio of each metabolite to IS versus analyte concentration. The linearity was evaluated by the correlation coefficient (*r*<sup>2</sup>). According to the signal-to-noise ratio provided by the Leco ChromaTOF program (version 3.30, Leco, St. Joseph, MI, USA), the limit of detection (LOD) was calculated for the minimum concentration of each test compound with a signal to noise ratio of 3:1.

The accuracy and precision of the ultrasonic method were determined by calculating the relative standard deviation (RSD) and the peak-area ratios of selected metabolites to IS from serum samples and standards tested. The intraday precision and the interday precision of the 40 standards were assessed within 24 h and for six consecutive days, respectively. Also, the reproducibility was evaluated by independently preparing serum samples six times within 24 h. In addition, the stability of the same serum samples was evaluated in period of 72 h. The recovery was determined by the addition of standard compounds at three different concentrations to 100 μL of serum samples.

**Table 1:** Orthogonal experimental design for optimizing the derivatization conditions

Experiment	Derivatization temperature (°C)	Reaction time (min)	Ultrasonic irradiation (40 kHz, 350 W) (%)	BSTFA+1% TMCS (μL)	<i>n</i> -Hexane (μL)
N01	35	5	100	100	20
N02	35	10	100	60	60
N03	35	15	100	80	40
N04	50	5	100	60	60
N05	50	10	100	80	40
N06	50	15	100	100	20
N07	65	5	100	80	40
N08	65	10	100	100	20
N09	65	15	100	60	60
N10	35	5	70	80	40
N11	35	10	70	100	20
N12	35	15	70	60	60
N13	50	5	70	100	20
N14	50	10	70	60	60
N15	50	15	70	80	40
N16	65	5	70	60	60
N17	65	10	70	80	40
N18	65	15	70	100	20
N19	35	5	40	60	60
N20	35	10	40	80	40
N21	35	15	40	100	20
N22	50	5	40	80	40
N23	50	10	40	100	20
N24	50	15	40	60	60
N25	65	5	40	100	20
N26	65	10	40	60	60
N27	65	15	40	80	40
N28 <sup>a</sup>	70	15	0	80	40
N29 <sup>a</sup>	70	60	0	80	40

BSTFA *N,O*-bis(trimethylsilyl)trifluoroacetamide, TMCS trimethylchlorosilane

<sup>a</sup>Conventional silylation method as control.

### Data processing and statistical analysis of GC/TOFMS

As described in a previous study [11], the samples were analyzed by GC/TOFMS using L-2-chlorophenylalanine as an IS for batch quality control, and heptadecanoic acid for the data processing of fatty acids. In addition, L-2-chlorophenylalanine and heptadecanoic acid were utilized to assess process variability during sample preparation and data processing. Metabolite identification was performed by ChromaTOF coupled with National Institute of Standards and Technology (NIST) spectral library databases (2005). Authentic reference standards were used to further validate identified metabolites.

The acquired dataset in MS files from GC/TOFMS analysis was exported into NetCDF format by ChromaTOF. CDF files were processed using custom scripts (revised MATLAB toolbox, hierarchical multivariate curve resolution (H-MCR), developed by Jonsson et al. [24, 25]) in MATLAB 7.0 (The MathWorks) including baseline correction, denoising, smoothing, time-window splitting, multivariate curve resolution (identification of overlap peaks), and alignment. The resulting three-dimensional dataset comprised sample information, peak retention time, and peak intensity. Some artificial peaks generated by noise, column bleed, and by-products in the silylation procedure were removed manually from the dataset. The resulting data were normalized to the area of the IS (IS peaks were removed afterward), mean-centered, and then treated by unit variance scaling for further statistical analysis. Principal component analysis (PCA), projection to latent structures (PLS), or orthogonal projection to latent structures (OPLS) was carried out using the SIMCA-p 12.0 software package (Umetrics, Umeå, Sweden) to

visually display the correlation between the experimental parameters and metabolic information. The following statistics, based on the models, are discussed in detail throughout this article:  $R^2X$  is the cumulative modeled variation in the X matrix;  $R^2Y$  is the cumulative modeled variation in the Y matrix; and  $Q^2Y$  is the cumulative predicted variation in the Y variable or matrix, according to sevenfold cross-validation. The range of these parameters is 0-1, where 1 indicates a perfect fit.

## RESULTS AND DISCUSSION

### *Ultrasonication-assisted conditions*

**Optimization of ultrasonication extraction time.** PLS analysis enabled a practical assessment of metabolite extraction efficiency of different extraction times under ultrasonication. In Fig. 1, the PLS loading plot with three components ( $R^2X = 0.360$ ,  $R^2Y = 0.838$ , and  $Q^2 = 0.258$ ; explained 83.8% and predicted 25.8% of the variation in the resolved peak areas) indicated the inner correlation structure between the metabolite intensity (peak areas) matrix X and the condition matrix Y. The X matrix comprises red boxes Fig. 1, which denote the ten ultrasonic time points in duplicates and two vortex times in duplicates. The Y matrix comprises black triangles in Fig. 1, denoting the areas of the resolved 570 GC/TOFMS peaks. The areas of resolved peaks corresponding to different extraction time points determined the distribution of experimental samples on the PLS loading plot. All major peaks had a significant positive effect when the ultrasonic extraction time was set as 3–10 min, especially at 4 min. In addition, the results of all duplicates at 1–10 min showed good reproducibility in the PLS loading plot. However, a long ultrasonic extraction time of 15–30 min resulted in decreased reproducibility. These results indicate that the overall extraction efficiency of the conventional vortex method at 2 and 10 min was not as good as the ultrasonic extraction method, particularly in comparison with the results with an ultrasonic extraction time of 4 min. Also, it is advisable to have a relatively short ultrasonication time for improved extraction efficiency.

We compared the identified compounds obtained from the ultrasonic method with those obtained from the conventional vortex method. Most of these compounds (e.g., allantoin, alanine, hexadecanoic acid, and fructose) positively correlated with ultrasonic extraction methods, whereas only a small number of metabolites (e.g., uric acid, citrate acid, and glucosamine) correlated with conventional vortex methods (see Fig. S1). Therefore, we believe that in comparison with conventional vortexing, ultrasonication significantly enhanced the metabolite extraction efficiency.

**Optimization of ultrasonicated methoxymation.** The methoxymation method is performed prior to silylation [26] to reduce multiple-peak formation of individual sugars owing to the various types of structures, such as open chain or cyclic structure, and to stabilize the carbonyl moieties in the aldose or ketose. In this study, the peak-area of the glucose cyclic trimethylsilyl (TMS) derivative to the glucose methoxime/TMS derivative is considered an indicator of methoxymation efficiency. The lower the peak-area ratio of two different glucose forms, the higher the methoxymation efficiency of glucose. As shown in Fig. 2, when the peak-area ratio decreased with the 20–45 min reaction time, the methoxymation efficiency of the ultrasonic method was better than that of the conventional method, with relatively low standard deviations (below 0.003). However, a 60 min reaction time resulted in a high peak-area ratio. This is because that derivatization efficiency may be inhibited by a prolonged derivatization time.

Accordingly, 20 min was considered as the most suitable condition for methoxymation under ultrasonication.

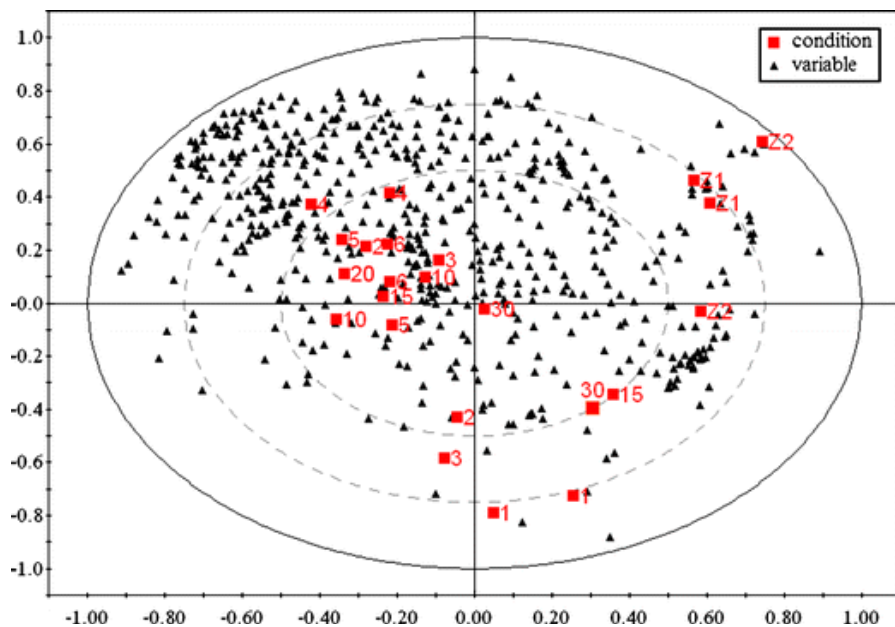


**Figure 1:** Study of the optimal ultrasonic time for extracting the metabolites in human serum. The projection to latent structures (PLS) biplot shows the correlation between the variable (peak areas) and conditions (extraction time). Ultrasonic extraction was carried out for 1, 2, 3, 4, 5, 6, 10, 15, 20, and 30 min (labeled as *numerals*), respectively. Conventional extraction was vortexed for 2 and 10 min (labeled as *Z1* and *Z2*), respectively. Each experimental condition was duplicated. The optimal condition influencing the peak areas is 4 min, which is positively correlated to most of the resolved peaks

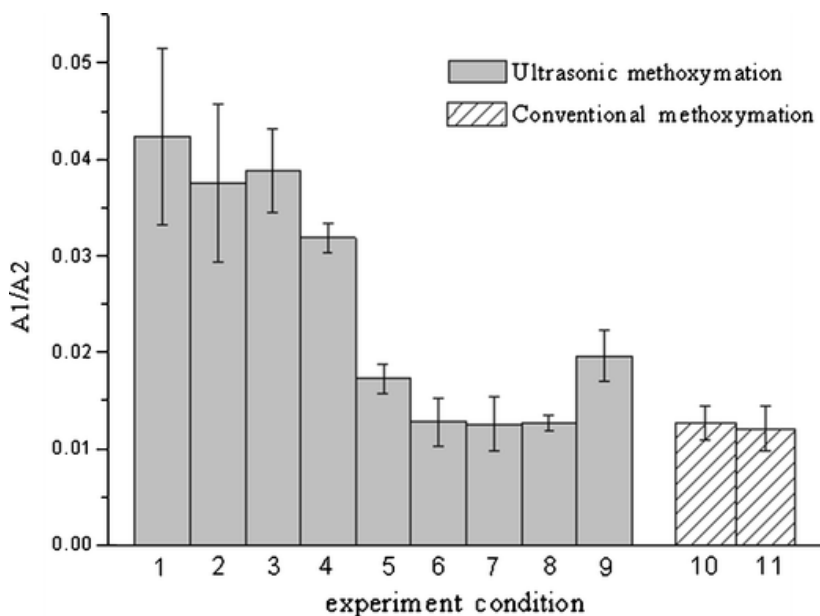


**Figure 2:** Effect of the ultrasound-enhanced methoxymation protocol and conventional methoxymation method for analysis of glucose in the serum sample. *A1* the peak area of the glucose cyclic trimethylsilyl (TMS) derivative, *A2* the peak area of the glucose methoxime/TMS derivative. *Error bars* illustrate the standard deviation ( $n = 3$ ). The

ultrasonic times (columns 1–9) were 2, 5, 7, 10, 15, 20, 30, 45, and 60 min, respectively; conventional methoxymation times as a control (columns 10 and 11) were 1.5 and 16 h

**Optimization of ultrasonicated silylation.** We used an orthogonal experimental design  $L_{27}(3^{13})$  to investigate the influence of different factors (ultrasonic irradiation power, ultrasonic time, temperature, silylation volume, and solvent volume) on the efficiencies of silylation of metabolites from human serum samples. A three-component PLS model was established, with the parameters  $R^2X$  (0.459),  $R^2Y$  (0.624), and  $Q^2$  (0.372), for correlating the 29 experimental conditions (X matrix) to the areas of 431 peaks (Y matrix). A score-loading biplot (Fig. 3a) was constructed to visualize the relationship between factors, variables (resolved peak areas), and conditions (see Table 1). It can be seen in Fig. 3a that most of the variables clustered in the middle, drifted slightly to the right, and thus are considered positively correlated to three of the five factors: ultrasonic irradiation power, ultrasonic time, and silylation volume. Compared with the other factors, temperature and *n*-hexane have less effect on the resolved peak areas, and thus contribute less to the extraction and silylation efficiency. Experimental conditions labeled as N06, N11, N13, and N08 are located close to most of the variables (Fig. 3a), suggesting that these four conditions affect the silylation efficiency to a greater extent than the others. In the  $t1-u1$  scores plot (Fig. 3b) of the PLS model, the four experimental conditions cluster in the upper-right quadrant, which may correlate to relatively higher peak areas. Additionally, experimental condition N08 (two samples), located at the upper-right corner, appears to be associated with the maximum peak intensity.

To validate the above conclusion and to further compare the new methods (N06 and N08) with the conventional conditions (N28 and N29), another PLS model using 145 identified metabolites and eight samples was generated (three components,  $R^2X = 0.935$ ,  $R^2Y = 0.998$ , and  $Q^2 = 0.964$ ). The relative positions of the five factors in the biplot (Fig. 3c) are consistent with those of Fig. 3a. This confirms that the three factors (ultrasonic irradiation power, ultrasonic time, and silylation volume) may strongly affect the peak areas of the identified metabolites. The experiments with the new ultrasonic (N06 and N08) and conventional thermal (N28 and N29) conditions locate separately with large intergroup and small intragroup distances. Comparatively, N08 is positively correlated to a higher peak area of the metabolites, showing an enhancement for the silylation reaction. On the basis of the above results, the optimized ultrasonic condition is considered to be 100% irradiation amplitude (450-W power of the nominal converter), 100  $\mu$ L BSTFA (1% TMS), 20  $\mu$ L *n*-hexane, and 65 °C for 10 min. The short derivatization time, which was only 10 min, will enable a high-throughput profiling of human biological samples.

In addition, the ultrasonication used in the method enhanced the derivatization efficiency, as evidenced by the enhanced peak intensity for most metabolites in the human serum sample, involving different classes of metabolites, including amino acids, organic acids, fatty acids, and carbohydrates. The peak intensity of 16 amino acids was increased by 8.0–92.1% (Table S1). About 50% of these amino acids increased their peak intensity by 14.0% or more. It is worth noting that some amino acids may undergo chemical conversions (e.g., glutamine converts to glutamic acid) during the silylation process [27]. However, our present study indicated that the peak intensity of glutamine increased by 92.1% with the aid of ultrasonication, suggesting that the chemical conversion is minimized owing to the enhanced silylation. At the levels of number of keto-containing organic acids (e.g.,  $\alpha$ -ketoglutaric acid, pyruvate, 3-methyl-2-oxobutyric acid,



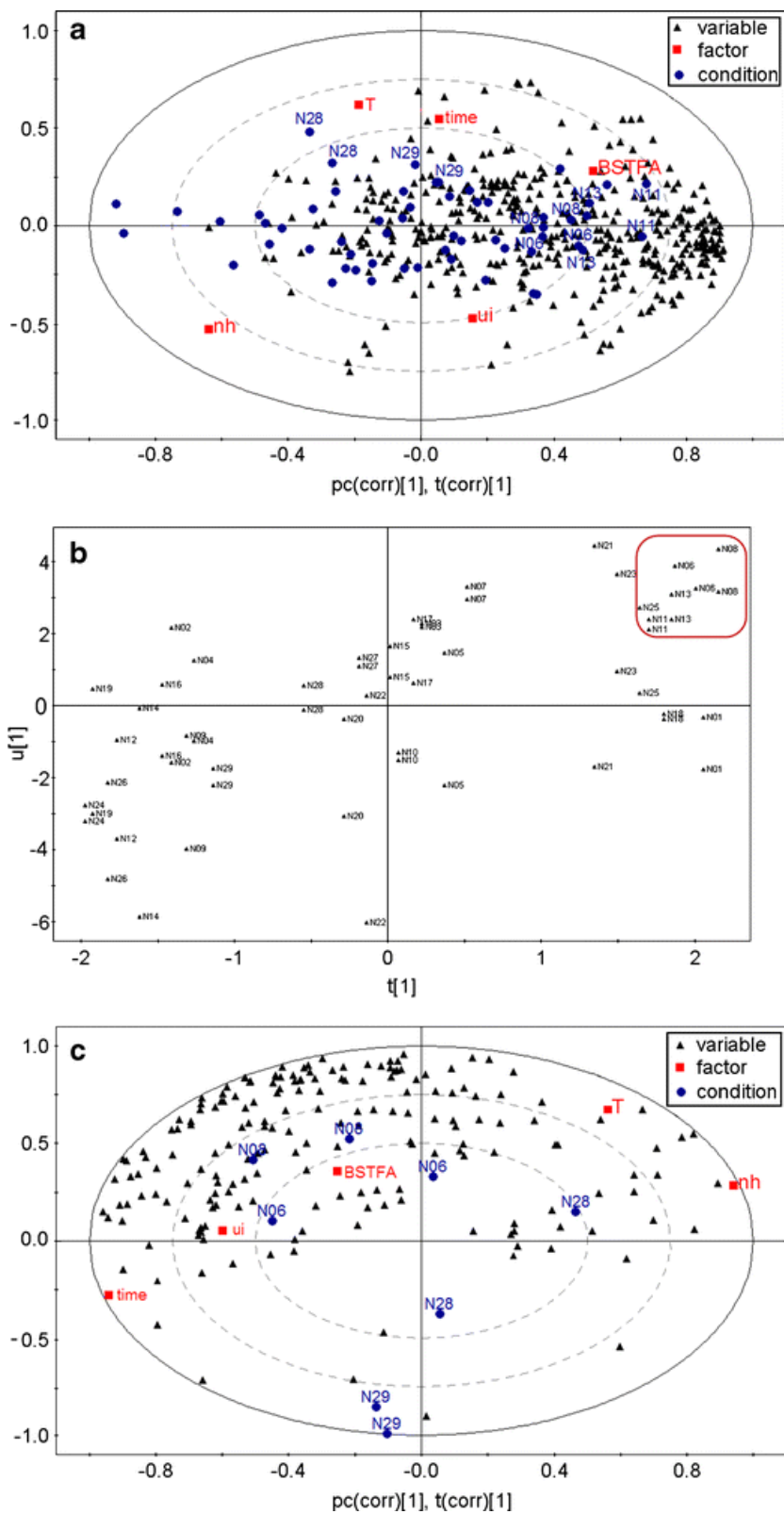


**Figure 3:** Results from the optimization of the ultrasonication-assisted derivatization condition (see Table 1 for details). **a** Score-loading biplot of gas chromatography/time-of-flight mass spectrometry data from the PLS model of serum samples shows the correlation among factors (temperature, ultrasonic irradiation power, ultrasonic time, silylation volume, and *n*-hexane; labeled as *T*, *ui*, *time*, *BSTFA*, and *nh*), variables (the areas of 431 resolved peaks),

and derivatization conditions (29 experiments, 58 samples). Typical data points representing experimental conditions are labeled. **b** The PLS scores plot (t1-u1) shows a strong correlation between the various derivatization conditions and the areas of the resolved peaks. Each experimental condition was performed in duplicate. **c** Score-loading biplot of the PLS model indicates the correlation between factors (temperature, ultrasonic irradiation power, ultrasonic time, silylation volume, and *n*-hexane; labeled as *T*, *ui*, *time*, *BSTFA*, and *nh*), variables (peak areas of 145 identified metabolites), and derivatization conditions (N06, N08, N28, and N29)

2-oxopentanoic acid, 3-methyl-2-oxopentanoic acid, and 2-oxohexanoic acid) in serum were significantly elevated by 17.1–59.8%. A possible reason is that increased “local” temperature and pressure generated from ultrasound activation at the interface between the cavity and the bulk liquid, via the collapsing bubble [28], may improve the chemical transformation of unstable metabolites, such as the keto–enol conversion in carbonyl-containing metabolites. In addition to organic acids, the levels of carbonyl-containing compound, including 3-amino-2-piperidone, creatinine, and hypoxanthine, were found at increased intensities. Therefore, ultrasonication may favor the silylation of unsaturated fatty acids with one or more double bonds, such as palmitelaidic acid, *trans*-9-octadecenoic acid, 9,12-octadecadienoic acid, and eicosenoic acid.

### Method validation

The discrepancy in results obtained from sera and standards is presumably due to the matrix effect [29]. The compositional difference between the standard compounds and human serum samples will be carried into TMS derivatization and subsequent gas-chromatographic separation, leading to discrepancies in quantitative results of metabolites obtained from the two sample matrices. We investigated the linearity and the correlation coefficients ( $r^2$ ) of reference standards and serum samples with the purpose of considering the matrix effect. We used 40 compounds representing different classes of metabolites for the validation. The  $r^2$  for the test compounds in reference standards at different concentrations approached 1.0000 with the IS adjustment. Analogously, the  $r^2$  for most of the test compounds in serum samples at different dilution levels were higher than 0.9940. Exceptions were glycine and citric acid, with poor correlation coefficients (Table 2). In addition, it was found in most cases that the LODs were in the range from 0.03 to 0.8  $\mu\text{M}$ . Higher LODs were also found within the range from 1.6 to 4.7  $\mu\text{M}$  for  $\alpha$ -ketoglutaric acid, maleic acid, histamine, glutamine, eicosanoic acid, estrone, and testosterone. This finding suggests that the ultrasonic derivatization method is acceptable for large-scale sample profiling, as evidenced by the fact that different classes of metabolites in the standard samples and serum samples show good linearity and sensitivities, as compared with previously reported methods [8, 13].

The quantitative method was validated in terms of accuracy and precision (Table 3). The intraday and interday RSDs of the standard compounds were in the range from 3.4 to 14.6% ( $n = 6$ ) and from 2.1 to 14.9% ( $n = 6$ ), respectively. The results of the same 40 compounds in the serum samples tested indicated that the derivatized samples were stable for 72 h, with RSDs of less than 10.0%. Reproducibility also showed acceptable results, with relatively low RSDs (15.3% or less) for most of the identified compounds in the six duplicate serum samples tested by two different operators in our laboratory. However, poor precision and reproducibility were observed with estrone and testosterone. Furthermore, the recoveries of three different concentrations of the 39 compounds ranged from 70.0 to 118.9%, with RSDs less than 15.5%, except for succinic acid, with recoveries ranging from 61.1 to 75.7%. These results indicate that

**Table 2:** Linearity and limit of detection (*LOD*) of reference standards and serum metabolites

Compound	Linear range of standards <sup>a</sup> ( $\mu\text{g}\cdot\text{mL}^{-1}$ )	<i>n</i>	<i>r</i> <sup>2b</sup>	Linear range of serum samples <sup>c</sup> (v/v)	<i>n</i>	<i>r</i> <sup>2b</sup>	LOD ( $\mu\text{M}$ ) <sup>d</sup>
L- $\alpha$ -Alanine	0.25–125.0	8	0.9991	0.3–1	8	0.9991	0.03
L-Valine	0.25–125.0	8	0.9985	0.3–1	8	0.9969	0.04
L-Isoleucine	0.25–125.0	8	0.9996	0.3–1	8	0.9976	0.04
L-Proline	0.25–125.0	8	0.9963	0.3–1	8	0.9987	0.04
Glycine	0.25–125.0	8	0.9991	0.3–1	8	0.9845	0.14
L-Serine	0.25–125.0	8	0.9975	0.3–1	8	0.9994	0.05
L-Threonine	0.25–125.0	8	0.9964	0.3–1	8	0.9994	0.07
L-Aspartic acid	0.25–125.0	8	0.9969	0.3–1	8	0.9975	0.3
L-Methionine	0.25–125.0	8	0.9992	0.3–1	8	0.9985	0.1
4-Aminobutanoic acid	0.25–125.0	8	0.9997	0.3–1	8	0.9975	0.1
Histamine	5.0–125.0	6	0.9931	0.3–1	8	0.9988	4.7
Glutamine	5.0–625.0	7	0.9990	0.3–1	8	0.9961	4.1
L-Asparagine	0.25–125.0	8	0.9978	0.3–1	8	0.9992	0.2
L-Ornithine	2.5–125.0	8	0.9997	0.3–1	8	0.9971	0.1
L-Histidine	0.25–125.0	8	0.9963	0.3–1	8	0.9991	0.2
L-Lysine	0.25–125.0	8	0.9984	0.3–1	8	0.9987	0.3
L-Tyrosine	2.5–125.0	8	0.9954	0.3–1	8	0.9950	0.3
L-Tryptophan	2.5–125.0	8	0.9943	0.3–1	8	0.9956	0.4
Uridine	2.5–125.0	8	0.9935	0.3–1	8	0.9964	0.08
Maleic acid	2.5–125.0	6	0.9982	0.3–1	8	0.9962	2.3
Succinic acid	0.25–125.0	7	0.9951	0.3–1	8	0.9980	0.04
Fumaric acid	2.5–125.0	8	0.9984	0.3–1	8	0.9956	0.1
$\alpha$ -Ketoglutaric acid	2.5–125.0	8	0.9993	0.3–1	8	0.9974	1.6
Citric acid	2.5–125.0	8	0.9964	0.3–1	8	0.9898	0.8
Ribitol	0.25–125.0	8	0.9942	0.3–1	8	0.9972	0.1
D-Fructose	2.5–125.0	8	0.9983	0.3–1	8	0.9991	0.1
D-Gluconic acid	0.25–125.0	8	0.9953	0.3–1	8	0.9992	0.3
Tetradecanoic acid	2.5–125.0	8	0.9946	0.3–1	8	0.9976	0.1
Palmitelaidic acid	0.05–12.50	8	0.9937	0.3–1	8	0.9995	0.03
Hexadecanoic acid	0.25–125.0	8	0.9979	0.3–1	8	0.9961	0.04
Linoleic acid	0.05–12.5	7	0.9963	0.3–1	8	0.9963	0.06
Oleic acid	0.25–125.0	8	0.9938	0.3–1	8	0.9945	0.06
<i>trans</i> -9-Octadecenoic acid	0.25–125.0	8	0.9988	0.3–1	8	0.9987	0.05
Octadecanoic acid	2.5–125.0	8	0.9964	0.3–1	8	0.9944	0.05
Arachidonic acid	0.05–12.5	7	0.9970	0.3–1	8	0.9961	0.09
Eicosapentaenoic acid	0.05–12.5	8	0.9977	0.3–1	8	0.9954	0.04
Eicosanoic acid	2.5–125.0	8	0.9965	0.3–1	8	0.9953	2.0
Docosahexenoic acid	0.25–125.0	8	0.9986	0.3–1	8	0.9958	0.08
Estrone	2.5–125.0	7	0.9942	0.3–1	8	0.9978	1.5
Testosterone	2.5–125.0	6	0.9986	0.3–1	7	0.9959	1.3

<sup>a</sup>Reference standards for each amino acid, organic acid, nucleoside, and carbohydrate at different concentrations were diluted with water.

Reference standards for each fatty acid and cholesterol at different concentrations were diluted with methanol.

<sup>b</sup>Correlation coefficients were determined at the range of concentrations listed here.

<sup>c</sup>A series of diluted serum samples at relative concentrations of 0.3, 0.4, 0.5, 0.6, 0.7, 0.8, 0.9, and 1.0 (v/v, serum/serum + water) were prepared with the corresponding procedure.

<sup>d</sup>The LOD was calculated from the analysis of reference standards with a signal-to-noise ratio of 3:1.

the stability, reproducibility, and recovery of most of the compounds in serum samples were satisfactory, with the exception of several compounds such as succinic acid, estrone, and testosterone. As expected, most of the test compounds were not affected by the matrix effect of serum under the ultrasonic derivatization. The rationale for the use of 40 test compounds in this study is that they covered the major classes of metabolites, including amino acids, organic acids, fatty acids, nucleosides, carbohydrates, and cholesterols, exhibiting great diversity in molecular weight, polarity, and metabolic pathways involved. Thus, we conclude that the proposed ultrasonic method is stable and reliable for quantitative measurement of a wide array of metabolites with various chemical characteristics, and can be used for the metabolomic analysis of biological samples.

**Table 3:** Precision, reproducibility, stability, and recovery of the test compounds

Compound	Precision		Reproducibility	Stability	Recovery (%) $n = 3$					
	Intraday precision <sup>a</sup>	Interday precision <sup>a</sup>			1 <sup>b</sup>		2 <sup>c</sup>		3 <sup>d</sup>	
	RSD (%) $n = 6$	RSD (%) $n = 6$	RSD (%) $n = 6$	RSD (%) $n = 6$	Average	RSD	Average	RSD	Average	RSD
L- $\alpha$ -Alanine	7.1	5.1	6.8	4.4	96.1	7.6	113.4	10.9	118.9	5.5
L-Valine	7.0	5.4	8.6	4.9	93.0	15.3	93.5	1.1	94.2	5.3
L-Isoleucine	6.4	6.0	8.1	4.9	80.1	7.9	86.3	1.8	92.5	2.1
L-Proline	6.7	5.4	4.8	1.5	96.3	8.1	115.8	8.7	110.9	11.7
Glycine	4.6	11.7	13.1	1.1	114.9	0.6	133.7	8.5	118.9	2.4
L-Serine	6.1	5.8	2.0	1.5	82.6	5.7	86.2	7.2	89.9	9.1
L-Threonine	5.0	4.7	1.8	1.2	91.7	14.3	91.1	7.8	93.8	6.6
L-Aspartic acid	4.5	6.7	4.7	3.2	74.6	2.4	72.4	7.9	82.9	6.3
L-Methionine	4.8	9.0	9.1	4.7	88.6	8.0	97.5	2.20	101.3	6.8
4-Aminobutanoic acid	4.7	9.5	1.2	0.6	70.0	12.8	79.1	3.4	92.2	1.5
Histamine	4.1	9.2	11.1	6.9	96.9	6.3	76.2	6.6	77.2	4.7
Glutamine	10.1	14.5	4.1	2.1	92.9	7.6	113.6	9.0	83.7	11.9
L-Asparagine	4.1	2.5	3.8	0.4	72.3	6.1	70.2	10.4	75.8	7.0
L-Ornithine	3.4	10.0	7.3	6.6	74.8	13.5	78.4	3.1	85.3	5.9
L-Histidine	5.2	5.1	6.4	3.8	99.1	7.2	92.4	2.74	91.6	6.4
L-Lysine	3.8	7.1	10.9	3.4	109.1	10.4	114.9	14.6	102.8	10.2
L-Tyrosine	5.9	2.5	4.6	1.7	77.3	7.7	82.7	12.0	88.1	7.6
L-Tryptophan	4.7	7.4	2.0	2.1	101.4	11.1	103.0	7.4	100.2	7.9
Uridine	11.3	13.2	5.1	4.1	98.2	5.8	102.1	5.6	102.6	4.7
Maleic acid	8.9	6.0	15.3	3.1	76.7	4.3	81.0	5.7	74.3	7.2
Succinic acid	5.2	3.9	2.6	2.6	66.2	10.4	61.1	5.7	75.7	7.4
Fumaric acid	7.3	11.9	13.6	7.1	92.7	3.3	96.1	5.5	89.4	7.3
$\alpha$ -Ketoglutaric acid	4.0	12.1	5.3	1.6	85.9	1.22	109.9	6.9	108.1	4.3
Citric acid	9.1	7.6	1.7	2.4	92.1	12.8	76.8	4.7	86.2	5.5
Ribitol	6.3	4.4	1.8	0.4	97.3	6.7	92.9	4.2	97.5	3.8
D-Fructose	12.6	7.0	3.1	2.1	114.1	8.4	106.2	5.0	86.0	15.5
D-Gluconic acid	14.0	9.9	5.7	1.7	112.0	4.8	113.9	1.0	115.5	1.6
Tetradecanoic acid	11.9	2.1	2.4	0.2	105.4	14.2	117.0	4.8	117.9	2.9
Palmitelaidic acid	10.7	4.3	0.6	0.4	82.8	4.1	89.3	1.3	92.2	3.6
Hexadecanoic acid	10.3	3.0	2.0	3.0	114.3	8.50	118.0	0.5	118.5	0.8
Linoleic acid	10.3	6.0	2.9	2.7	96.9	1.9	101.4	0.9	98.0	3.5
Oleic acid	9.8	5.2	1.4	0.1	100.1	2.9	102.6	1.2	100.9	3.7
<i>trans</i> -9-Octadecenoic acid	9.8	5.7	1.3	1.0	90.4	1.5	96.1	0.8	99.2	2.7
Octadecanoic acid	9.4	5.2	3.2	2.2	104.1	3.7	115.4	2.3	116.5	0.5
Arachidonic acid	10.3	5.7	2.6	2.3	97.4	6.8	96.4	1.4	99.9	2.2
Eicosapentaenoic acid	9.7	6.1	0.8	0.7	85.0	3.1	93.7	0.5	95.0	1.9
Eicosanoic acid	14.6	14.9	4.8	5.8	104.5	1.9	92.8	2.2	97.4	2.1
Docosahexenoic acid	10.2	7.9	0.9	0.7	98.1	5.5	98.3	1.2	99.0	5.1
Estrone	23.3	18.8	4.9	11.1	108.3	1.15	107.5	11.5	109.5	3.3
Testosterone	16.3	9.0	5.8	23.4	82.5	11.3	88.6	5.2	91.9	5.2

<sup>a</sup>The intraday precision and interday precision of the test standard for each amino acid, organic acid, and carbohydrate ( $9.37 \mu\text{g mL}^{-1}$ ) and for each fatty acid and cholesterol ( $18.75 \mu\text{g mL}^{-1}$ ).

<sup>b</sup>Recovery of a low concentration of the added test standard ( $6.25 \mu\text{g mL}^{-1}$ ) in the serum sample

<sup>c</sup>Recovery of a middle concentration of the added test standard ( $12.50 \mu\text{g mL}^{-1}$ ) in the serum sample

<sup>d</sup>Recovery of a high concentration of the added test standard ( $18.75 \mu\text{g mL}^{-1}$ ) in the serum sample

### Comparison between the ultrasonic and conventional methods for serum samples

To evaluate the ultrasonic derivatization, serum samples obtained from ten healthy individuals were prepared with the ultrasonic and conventional methods respectively and the GC/TOFMS data obtained were processed using the H-MCR method. Although some metabolites were qualitatively confirmed in previous publications [8, 13], the current method identified more kinds of metabolites. After the matrix interference (e.g., false peak, silicone bleeding) had been eliminated, 145 metabolites from the resolved peaks detected in the total ion chromatograms of

serum samples prepared by the ultrasonic method were annotated using reference standards and the NIST spectral library (see Table S2).

Additionally, the ultrasonication-aided derivatization of human serum metabolites yielded about the same number of original peaks as the conventional method (663 vs. 656), but with higher intensity of 64.0% of the peaks, suggesting the improved derivatization efficiency with ultrasonication. Among the 145 identified peaks, 71.0% peaks were found with significantly increased intensity, among which 5.5% increased by 3 times or more, 2.8% increased by 2–3 times, 29.0% increased by 1.2–2 times, and 33.8% increased by 1–1.2 times. About 26.2% of the 145 peaks were found with slightly decreased intensity, and only 2.8% were found with a maximum decreased rate of less than 4 times (Fig. 4). Also, the ultrasonic method has an effect similar to that of the conventional derivatization method on the formation of methoxime, as evidenced by the similar mean peak-area ratio of the glucose cyclic TMS derivative to the glucose methoxime/TMS derivative obtained from the two methods (data not shown).

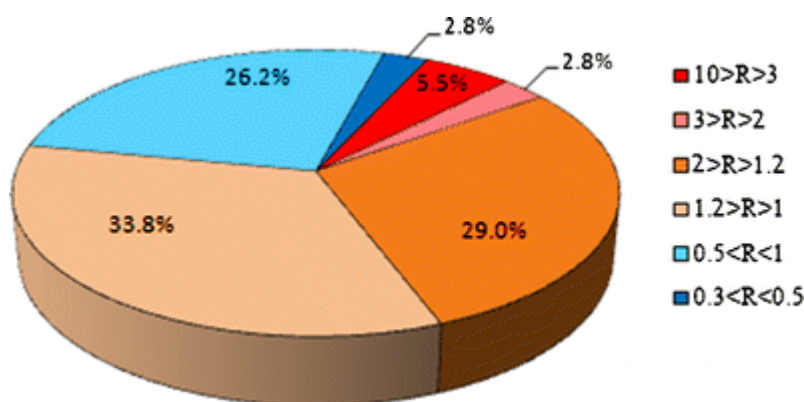


**Figure 4:** A pie chart for the ratio of the components with the peak intensity increased and decreased in the ultrasonic derivatization compared with the conventional derivatization. The comparison ratio was calculated with the equation  $R$  (ratio) =  $A\%/B\%$ , in which  $A\%$  represents the mean peak-area ratio of each component to the internal standard (IS) in serum samples prepared by the ultrasonic method and  $B\%$  represents the mean peak-area ratio of each component to the IS in serum samples prepared by the conventional method

Importantly, the ultrasonication-aided derivatization process involving methoxymation and silylation was completed within approximately 30 min. Compared with the 3 h methoxymation and 17 h silylation in the conventional method [11, 13], the new approach allowed a much faster process, which is particularly attractive for high-throughput metabolomic studies.

### Application

An epidemiological study showed that hypertension is the primary risk factor for cardiovascular disease worldwide [30]. Metabolomics has shown great potential in advancing our understanding of the pathophysiological processes of hypertension in rat models [10, 31–34]. However, there are very few publications directly related to the global metabolic profiling of human blood, except for two that investigated the relationship between blood lipids and blood pressure [35, 36]. We applied the new ultrasonic derivatization technology to analyze serum samples obtained from 34 elderly hypertensive patients and 29 healthy individuals. There were no significant differences between the two groups in age, body mass index, and gender. The typical total ion

chromatograms of serum samples showed some obvious differences between the two groups (see Fig. S2).

The unsupervised PCA model illustrated the clear separation between 34 hypertensive patients and 29 healthy counterparts (data not shown). Additionally, the metabolic profiles of the two groups were differentiated by an OPLS model (see Fig. S3). The two clusters of samples showed distinct separation from each other in the OPLS scores plot. The variance explained by the first and second components of the model are 21% and 19% for X (the MS data), and 69% and 22% for Y (the class variable), respectively, whereas the cumulative  $Q^2$  of the model is 87%. These results demonstrated that the multivariate statistical model is robust, with reliable predictability. A univariate analysis of the *t* test experiments was concurrently performed for the validation of the variable selection by the PCA and OPLS models. On the basis of the variable importance in the projection (VIP) values ( $VIP > 1.0$ ) in the OPLS and the *p* values ( $p < 0.05$ ) in the *t* tests for all metabolites, 38 metabolite markers were selected, including carbohydrates, lipids, amino acids, and amino ketones, in the hypertensive patients relative to the healthy controls (Table 4). Deregulations of purine metabolism, metabolism of free fatty acids, glucose metabolism, urea cycle, and metabolism of amino acids potentially associated with the hypertension condition were revealed.

As one of independent risk factors for hypertension [37], the levels of serum free fatty acids were found to be significantly elevated in the hypertensive patients compared with the healthy controls. Most fatty acids are stored as triglycerides in adipose tissue and are partially released into the blood pool. The degradation of glycerides is inhibited by the suppression of lipase release, regulating the release of fatty acid into the blood. Since the patients with metabolic syndrome including hypertensive conditions are closely associated with declined insulin response, the impaired insulin regulation in catabolism of triglycerides may result in the increase in the levels of serum fatty acids in the hypertensive patients [38]. In our study, the level of 1-stearoylglycerol, 1-palmitoylglycerol, and free fatty acids (e.g., oleic acid, eicosanoic acid, hexanoic acid, heptanoic acid, nonanoic acid) were significantly higher in the hypertensive patients compared with the healthy controls. Triglycerides were also found at higher levels in the hypertensive patients by an enzymatic assay. Interestingly, medium-chain fatty acids (such as hexanoic acid, heptanoic acid, and nonanoic acid) were observed at higher levels in serum. As far as we know, the higher serum levels of medium-chain fatty acids and monoglycerides in hypertensive patients has not been reported so far. A somewhat relevant publication reported that administration of medium-chain fatty acids/medium-chain triglycerides ( $C_6$ – $C_{12}$ ) does not seem to affect blood pressure, but is helpful to improve cardiac dysfunction [39]. Besides the elevated level of glucose confirmed by our study and previous reports, we detected changes of other monosaccharides and disaccharides in patients (Table 3), among which the levels of galactose, glucosamine, sorbose, sucrose, sorbitol, inosose, and *myo*-inositol were elevated, whereas those of fructose, cellobiose, and lactobionic acid were decreased. These results suggest that a dysregulated carbohydrate metabolism occurred in hypertensive patients, as evidenced by clinical observations that the development of hypertension is frequently accompanied by an increasing incidence of impaired glucose tolerance [40]. Uric acid, an independent predictor of hypertension used in the clinic [41], can be metabolized to allantoin and urea via purine metabolism. In our study, serum allantoin and urea were observed at higher levels in the patients, suggesting an upregulated urea cycle, which is consistent with the uric acid assay in the clinic .

**Table 4:** Significant metabolites identified from orthogonal projection to latent structures discriminant analysis modeling of the metabolic profiles of hypertensive patients and healthy control subjects

Metabolites	VIP <sup>a</sup>	FC <sup>b</sup>	P (t test) <sup>c</sup>
D-Fructose	2.3	0.3	$4.5 \times 10^{-18}$
D-Glucose	2.2	3.0	$4.3 \times 10^{-15}$
D-Galactose	2.0	2.4	$6.0 \times 10^{-8}$
Glucosamine	1.6	3.8	$1.2 \times 10^{-8}$
L-Sorbose	1.6	2.9	$6.3 \times 10^{-6}$
Sucrose	1.3	1.8	$7.3 \times 10^{-5}$
D-Cellobiose	1.3	0.4	$4.8 \times 10^{-5}$
D-Sorbitol	1.2	2.6	$4.6 \times 10^{-3}$
Inosose	1.1	1.9	$1.6 \times 10^{-3}$
Lactobionic acid	1.1	0.5	$4.7 \times 10^{-4}$
myo-Inositol	1.0	1.3	$1.5 \times 10^{-3}$
Glycerol 3-phosphate	2.1	0.5	$4.6 \times 10^{-13}$
Heptanoic acid	2.0	1.6	$6.4 \times 10^{-7}$
1-Stearoylglycerol	1.6	4.3	$2.5 \times 10^{-7}$
Oleic acid	1.5	1.4	$1.7 \times 10^{-9}$
1-Palmitoylglycerol	1.4	1.5	$2.6 \times 10^{-7}$
Nonanoic acid	1.3	1.3	$1.2 \times 10^{-2}$
Eicosanoic acid	1.2	1.3	$3.3 \times 10^{-4}$
Hexanoic acid	1.0	2.0	$7.4 \times 10^{-3}$
Pipecolic acid	1.8	1.6	$1.5 \times 10^{-5}$
L-Ornithine	1.8	1.5	$2.6 \times 10^{-6}$
L-Lysine	1.8	1.5	$1.0 \times 10^{-5}$
Pyroglutamic acid	1.5	1.3	$2.4 \times 10^{-3}$
L-Histidine	1.5	1.4	$2.3 \times 10^{-4}$
L-Alanine	1.4	1.2	$9.5 \times 10^{-3}$
Glutamine	1.4	1.4	$3.7 \times 10^{-3}$
L-Isoleucine	1.4	1.2	$1.8 \times 10^{-2}$
$\alpha$ -Amino adipic acid	1.3	1.7	$6.5 \times 10^{-3}$
N-Acetylglycine	1.3	1.8	$2.0 \times 10^{-3}$
L-Tyrosine	1.2	1.5	$5.3 \times 10^{-3}$
Homocysteine	1.2	1.3	$1.9 \times 10^{-2}$
L-Aspartic acid	1.2	1.6	$1.6 \times 10^{-2}$
Glutamic acid	1.1	1.4	$3.7 \times 10^{-2}$
L-Tryptophan	1.0	1.3	$1.5 \times 10^{-3}$
Allantoin	2.0	1.5	$1.3 \times 10^{-5}$
3-Amino-2-piperidone	1.7	1.5	$4.5 \times 10^{-5}$
Urea	1.3	1.5	$4.9 \times 10^{-3}$
2-Ketoglutaric acid	1.7	2.1	$2.7 \times 10^{-5}$
Fasting blood glucose <sup>d</sup>		1.1	$4.9 \times 10^{-3}$
Triglycerides <sup>e</sup>		1.5	$5.5 \times 10^{-3}$

<sup>a</sup>Variable importance in the projection (VIP) is the relative influence of each metabolite on the grouping; metabolites with higher VIP values are more influential.

<sup>b</sup>Fold change (FC) is the ratio of the mean value for measured serum samples obtained from the hypertensive patient group to the mean value for the control samples obtained from the healthy subject group.

<sup>c</sup>P was calculated with Student's t test.  $P < 0.05$  means statistical significance.

<sup>d</sup>Fasting blood glucose was determined using a conventional glucose oxidase - peroxidase method.

<sup>e</sup>Triglycerides were determined by enzymatic assay.

evaluation of hypertension. Homocysteine is regarded as an independent risk factor for heart disease in older adults [42]. Our observation of the elevated homocysteine level in elderly hypertensive patients is consistent with previous reports [43]. The other amino acids, such as isoleucine, alanine, and lysine, were also observed at higher expression levels in serum. The higher serum amino acid concentrations may be indicative of the disturbed nitrogen metabolism in hypertensive patients, which may, in turn, accelerate the urea cycle. The accelerated urea cycle was indicated by elevated allantoin and urea levels in serum, and was further confirmed by the increased level of other intermediates in the urea cycle such as aspartic acid, glutamine, and ornithine. As hypertension will apparently increase the burden of the blood vessels and glomerular filtrations in the kidney, the increased serum urea level may also correlate with

impaired renal function, which coincides with the increased prevalence of renal disease in elderly hypertensive patients [44]. Therefore, we reasonably inferred that the proposed GC/TOFMS-based metabolic profiling technology is able to characterize the metabolic disturbances associated with hypertension.

## CONCLUSION

In this study, a novel ultrasonication-assisted extraction and derivatization protocol was developed for GC/TOFMS-based high-throughput metabolite profiling. The protocol was optimized with parameters including 4 min for ultrasonic extraction, 20 min for ultrasonic methoxymation, 100% irradiation amplitude (40 kHz; 350 W power), 100  $\mu$ L BSTFA (1% TMS), and 65  $^{\circ}$ C for 10 min for ultrasonic silylation. Compared with the methods conventionally used for derivatization, the ultrasonic protocol significantly enhanced the derivatization efficiency of the detected metabolites in serum and drastically shortened the reaction time from hours to minutes. This is of considerable benefit for the high-throughput profiling of metabolites from different sample matrices. Finally, the successful utilization of this protocol in the analysis of serum samples from hypertensive patients highlights its potential for large-scale clinical and epidemiological metabolomic applications.

## ABBREVIATIONS

BSTFA	<i>N,O</i> -bis(trimethylsilyl)trifluoroacetamide
GC/MS	Gas chromatography/mass spectrometry
GC/TOFMS	Gas chromatography/time-of-flight mass spectrometry
H-MCR	Hierarchical multivariate curve resolution
IS	Internal standard
LC/MS	Liquid chromatography/mass spectrometry
LOD	Limit of detection
OPLS	Orthogonal projection to latent structures
PCA	Principal component analysis
PLS	Projection to latent structures
RSD	Relative standard deviation
TMCS	Trimethylchlorosilane
TMS	Trimethylsilyl
VIP	Variable importance in the projection

## ACKNOWLEDGEMENTS

*This study was financially supported by the National Basic Research Program of China (2007CB914700), National Comprehensive Technology Platforms for Innovative Drug R&D (2009ZX09301-007), the National Natural Science Foundation of China (30901997, 20775048), and the Natural Science Foundation of Shanghai in China (10ZR1414800). We thank Jiaqiang Li and Limin Sun for their help and advice.*

## REFERENCES

1. Nicholson JK, Lindon JC, Holmes E (1999) *Xenobiotica* 29:1181–1189
2. Nicholson JK, Wilson ID (2003) *Nat Rev Drug Discov* 2:668–676
3. Schnackenberg LK, Beger RD (2006) *Pharmacogenomics* 7:1077–1086
4. Lenz EM, Wilson ID (2007) *J Proteome Res* 6:443–458



5. Lin JC, Su MM, Wang XY, Qiu YP, Li HK, Hao J, Yang HZ, Zhou MM, Yan C, Jia W (2008) *J Sep Sci* 31:2831–2838
6. Hartmann M, Zimmermann D, Nolte J (2008) *In Vitro Cell Dev Biol Anim* 44:458–463
7. Qiu YP, Su MM, Liu YM, Chen MJ, Gu JJ, Zhang J, Jia W (2007) *Anal Chim Acta* 583:277–283
8. Tao X, Liu Y, Qiu Y, Lin J, Zhao A, Su M, Jia W (2008) *Anal Bioanal Chem* 391:2881–2889
9. Bao YQ, Zhao T, Wang XY, Qiu YP, Su MM, Jia WP, Jia W (2009) *J Proteome Res* 8:1623–1630
10. Lu Y, A J, Wang G, Hao H, Huang Q, Yan B, Zha W, Gu S, Ren H, Zhang Y, Fan X, Zhang M, Hao K (2008) *Rapid Commun Mass Spectrom* 22:2882–2888
11. Qiu YP, Cai GX, Su MM, Chen TL, Zheng XJ, Xu Y, Ni Y, Zhao AH, Xu LX, Cai SJ, Jia W (2009) *J Proteome Res* 8:4844–4850
12. Halket JM, Zaikin VG (2003) *Eur J Mass Spectrom* 9:1–21
13. Jiye A, Trygg J, Gullberg J, Johansson AI, Jonsson P, Antti H, Marklund SL, Moritz T (2005) *Anal Chem* 77:8086–8094
14. Avila NS, Capote FP, de Castro MDL (2007) *J Chromatogr A* 1165:158–165
15. Athanasios M, Georgios L, Michael K (2007) *Food Chem* 102:606–611
16. Goldsmith JR (1997) *Environ Health Perspect* 105:1579–1587
17. Ando T, Kimura T (2003) *Jpn J Appl Phys* 42:2897–2900
18. Li JT, Wang SX, Chen GF, Li TS (2005) *Curr Org Synth* 2:415–436
19. Rodrigues S, Mazzone LCA, Santos FFP, Cruz MGA, Fernandes FAN (2009) *Braz J Chem Eng* 26:361–366
20. Deng S, Gangadharmath U, Chang CWT (2006) *J Org Chem* 71:5179–5185
21. Orozco-Solano M, Ruiz-Jiménez J, de Castro MDL (2010) *J Chromatogr A* 1217:1227–1235
22. Fiamegos YC, Nanos CG, Stalikas CD (2004) *J Chromatogr B* 813:89–94
23. <http://health.people.com.cn/GB/26466/45830/45832/3279162.html>
24. Jonsson P, Gullberg J, Nordstrom A, Kusano M, Kowalczyk M, Sjostrom M, Moritz T (2004) *Anal Chem* 76:1738–1745
25. Jonsson P, Johansson AI, Gullberg J, Trygg J, A JY, Grung B, Marklund S, Sjöström M, Antti H, Moritz T (2005) *Anal Chem* 77:5635–5642
26. Pasikanti KK, Ho PC, Chan ECY (2008) *Rapid Commun Mass Spectrom* 22:2984–2992
27. Casal S, Oliveira MD, Ferreira MA (2000) *J Chromatogr A* 866:221–230
28. Stavarache C, Pocsan AM, Vinatoru M, Mason T (2003) *J Ultrason Sonochem* 10:49–53
29. Büscher JM, Czernik D, Ewald JC, Sauer U, Zamboni N (2009) *Anal Chem* 81:2135–2143
30. Chockalingam A, Campbell NR, Fodor JG (2006) *Can J Cardiol* 22:553–555
31. Akira K, Masu S, Imachi M, Mitome H, Hashimoto M, Hashimoto T (2008) *J Pharm Biomed Anal* 46:550–556
32. Huhn SD, Szabo CM, Gass JH, Manzi AE (2004) *Anal Bioanal Chem* 378:1511–1519
33. Akira K, Masu S, Imachi M, Hashimoto T (2005) *Hypertens Res* 28:425–430
34. Inagaki S, Noda T, Min JZ, Toyooka T (2007) *J Chromatogr A* 1176:94–99
35. Brindle JT, Nicholson JK, Schofield PM, Grainger DJ, Holmes E (2003) *Analyst* 128:32–36
36. Graessler J, Schwudke D, Schwarz PEH, Herzog R, Schevchenko A, Bornstein SR (2009) *PLoS ONE* 4:1–3
37. Kutzing MK, Firestein BL (2008) *J Pharmacol Exp Ther* 324:1–7

38. Fagot-Campagna A, Balkau B, Simon D, Warnet JM, Claude JR, Ducimetière P, Eschwège E (1998) *Int J Epidemiol* 27:808–813
39. Nagao K, Yanagita T (2010) *Pharmacol Res* 61:208–212
40. Tugrul A, Guldiken S, Ugur-Altun B, Arikani E (2009) *Yonsei Med J* 502:195–199
41. Zechner R, Strauss JG, Haemmerle G, Lass A, Zimmermann R (2005) *Curr Opin Lipidol* 16:333–340
42. Scott J, Weir DQ (1996) *J Med* 89:561–563
43. Sutton-Tyrrell K, Bostom A, Selhub J, Zeigler-Johnson C (1997) *Circulation* 96:1745–1749
44. Zandi-Nejad K, Luyckx VA, Brenner BM (2006) *Ann Rom Soc Cell Biol* 14:226–230